Sonoluminescence and the Prospects for Table-Top Micro-Thermonuclear Fusion

William C. Moss, Douglas B. Clarke, John W. White, and David A. Young

Lawrence Livermore National Laboratory
P. O. Box 808
Livermore, CA 94550
wmoss@llnl.gov

Abstract

Hydrodynamic simulations of a collapsing bubble show that pure D_2 cannot exhibit picosecond sonoluminescence, because of its large sound speed. The addition of D_2O vapor lowers the sound speed and produces calculated results consistent with experiments. A pressure spike added to the periodic driving amplitude creates temperatures that may be sufficient to generate a very small number of thermonuclear D-D fusion reactions in the bubble.

Keywords: Sonoluminescence, hydrodynamic simulations, thermonuclear fusion

Sonoluminescence involves the conversion of acoustical energy to optical energy. It arises from the nucleation, growth, and collapse of gas-filled bubbles in a liquid. Recent experimental advances by Gaitan[1,2] produced stable synchronous sonoluminescence from a single acoustically levitated air bubble, with unexpected spectral and temporal properties. Using Gaitan's method, Barber and Putterman[3] reported emissions from a single pulsating bubble that were synchronous with the periodic acoustic driving field, and had a measured pulse width $\leq 50\,\mathrm{ps}$. The emission spectra were consistent with a $\geq 2\,\mathrm{eV}$ black body radiator.[4] Numerical hydrodynamic simulations[5,6] suggested that shock waves are generated during the collapse of the bubble and that they are capable of producing the short measured pulse widths and the inferred high temperatures. Moss et. al[6] showed that (*i*) shock waves *and* a (realistic) stiff soft–sphere potential for the gas in the bubble are required for the short pulse widths; and (*ii*) the increased specific heat, due to the ionization of the gas in the bubble, mitigated the peak temperatures at the center of the bubble. They predicted that temperatures approaching one kilovolt ($10^7\,\mathrm{K}$) might be attained in the absence of ionization. These high predicted temperatures in a minimally ionized gas lead naturally to speculation about the possibility of obtaining micro-thermonuclear fusion in a bubble filled with deuterium gas. In this Letter, we show that by adding a "spike" to the typical sinusoidal driving pressure, a small but measurable number of thermonuclear neutrons may be generated by a sonoluminescing deuterium bubble.

We consider numerical simulations of the growth and collapse of a bubble containing: (a) pure deuterium; (b) a mixture of deuterium and deuterated water vapor; and (c) the same mixture as (b) plus a "spike" added to the sinusoidal drive. All other initial and boundary conditions are identical.

We assume spherical symmetry and consider the motion of a gas-filled bubble with initial radius R_o surrounded by a shell of deuterated water, whose outer radius is R_W. The gas and water are initially at atmospheric pressure, $P_o = 1\,\text{bar}$, in thermal equilibrium, and at rest. The outer radius of the water is driven by an oscillatory pressure $P_o - P_a \sin\omega t$. We calculate the bubble's response to only one cycle of the driving oscillatory pressure, that is, only one of the many growth and collapse cycles that the bubble experiences. A complete simulation of steady state sonoluminescence would require specifying many quantities, such as the flask dimensions and thickness, transducer locations, the driving frequency and pressure, liquid and gas compositions, viscosities, thermal conductivities, and surface tensions, etc., which is beyond the scope of this paper. Nevertheless, we assume the physics that governs the creation of any one of the steady state sonoluminescent flashes can be approximated adequately using typical values for R_o, R_W, ω, and P_a, because the bubble collapse is primarily an inertial effect of the liquid compressing the gas. Any set of parameters that produces a typical bubble radius, as a function of time, should be sufficient to supply the necessary inertial forces that generate the flash. The parameters we have chosen are typical, but not representative of any particular experiment. We used $R_o = 10\,\mu\text{m}$, $R_W = 3\,\text{cm}$, and $\omega = 2\pi(27.6\,\text{kHz})$.[7] The pressure amplitude $P_a = 0.4\,\text{bar}$ was chosen to yield a maximum bubble radius of $\approx 90\,\mu\text{m}$, so the ratio R_{max}/R_o is consistent with experimental data.[8]

In the absence of viscosity, surface tension, heat conduction, mass diffusion, and nonmechanical energy loss (radiation), the equations for the conservation of mass, momentum, and energy for the system are[9,10]

$$
\begin{aligned}
\frac{D\rho}{Dt} + \rho\nabla\bullet\mathbf{v} &= 0, \\
\rho\frac{D\mathbf{v}}{Dt} + \nabla(P+Q) &= 0, \quad \text{and} \\
\frac{D\varepsilon}{Dt} + (P+Q)\frac{DV}{Dt} &= 0,
\end{aligned}
\tag{1}
$$

where ρ, $\mathbf{v}$, $Q(|\nabla\mathbf{v}|^2)$, $P(\rho, T)$, $\varepsilon(\rho, T)$, and V are the density, velocity, artificial viscosity,[10] pressure, specific internal energy, and specific volume [ρ^{-1}], and $\frac{D}{Dt} \equiv \frac{\partial}{\partial t} + \mathbf{v} \bullet \nabla$. Artificial viscosity is a standard computational method that gives shocks a finite thickness, so infinite gradients do not develop. The deuterated water was described by a polynomial equation of state for water[11] whose reference density was scaled by 20/18 (the ratio of the molecular weights of D_2O and H_2O). The deuterium gas was described by an analytic model[6] that includes vibrational excitation, dissociation, ionization, and repulsive and attractive intermolecular potentials. It was constructed from a combination of data and theory and is believed to be valid for the domains of density and temperature in this calculation. The deuterium equation of state is

$$
P = R'T\rho(1 + m_D(1 + 2m_I)) + \frac{E_c\rho_o}{1 - \frac{3}{n}}\left[(\rho/\rho_o)^{\frac{n}{3}+1} - (\rho/\rho_o)^2\right] \quad \text{and}
$$

$$
\begin{aligned}
\varepsilon = {} & \left[\frac{5}{2}R'T + \frac{R'\Theta}{e^{\Theta/T} - 1}\right](1 - m_D) + m_D R'T_D + \frac{3}{2}R'T(2m_D)(1 + m_I) \\
& + 2m_D R' m_I T_I + \frac{E_c}{\frac{n}{3} - 1}\left[(\rho/\rho_o)^{\frac{n}{3}} - \frac{n}{3}(\rho/\rho_o)\right] + E_c\,,
\end{aligned}
\tag{2a}
$$

where

$$
m_k = 0.5[\tanh[7(T - 0.9T_k)/T_k] + \tanh[6.3]]
\tag{2b}
$$

and $R' = R/4.03$ is the gas constant for deuterium. The first term in the pressure equation accounts for the increase in pressure due to the dissociation of molecular deuterium $(0 \le m_D \le 1;\ T_D = 4.5\ \mathrm{eV})$ [12] and ionization of the deuterium atoms $(0 \le m_I \le 1;\ T_I = 13.6\ \mathrm{eV})$. We have approximated the detailed density and temperature dependence of these energies using the functional form for m_k ($k = D, I$) in Eq. (2b). We have chosen $n = 5$, which provides an accurate representation of the deuterium 0 K isotherm to 200 Mbar.[13] The density of solid deuterium at 0 K is $\rho_o = 0.202$ g/cc [14] and we have set the binding energy $E_c = 1.09 \times 10^{10}\ \mathrm{erg/g}$, to obtain a best fit. The first term in the energy equation includes vibrational contributions ($\Theta = 4394$ K)[12] to the energy of a rigid diatomic molecule ($\gamma = 7/5$), where $\gamma \to (9/7)$ for $T >> \Theta$. We neglect the vibrational zero–point energy. The second term is the energy to dissociate a molecule, weighted by the dissociation fraction. The third term is the translational energy of the atoms and electrons. The fourth term is the ionization energy. The remaining terms are the potential energy. These terms are necessary for the gas equation of state to represent accurately dissociation, ionization, and both the repulsive and the attractive intermolecular potentials. Simpler models,[5] such as a van der Waals equation of state with a constant specific heat, are not valid at the densities and the temperatures that are reached during the final stages of the collapse of the bubble.

The equations of motion [Eq. (1)] and the equations-of-state [Eq. (2)], combined with the boundary and initial conditions given above comprise a complete set of equations that can be solved for the radial and temporal variation of all the field quantities. We solved numerically the differential equations incrementally in time, using a finite difference method. The water and the gas are divided into a mesh consisting of many concentric shells (zones) of fixed mass. The mass may vary from one shell to another. There must be enough shells to ensure that the finite difference solution converges to the differential equation solution. The zoning was identical in the three simulations: 600 equally sized gas zones (0.0167 μm/zone) and 960 water zones that increased geometrically in size from 0.000193 μm/zone at R_o, to 20 μm/zone at $R = 0.165$ cm, followed by 1417 equally sized zones (20 μm/zone) to R_W.

Figure 1a shows the calculated time dependence of the temperature at the center of the bubble, near the conclusion of the collapse of the pure deuterium bubble. The final 1.8 ns are shown, beginning at 38.2956 μs. The peak temperature is ≈ 0.5 eV, and the pulse width is ≈ 1 ns. The minimum bubble radius (0.5 μm) occurs at the same time as the peak temperature. This coincidence and the broad pulse suggest that either a shock has not formed, because the $n = 5$ potential in Eq. (2) is too soft, or the shock has formed too late in the implosion to have a significant effect. Figure 2 (solid line) shows the interface Mach number during the collapse, beginning at $R = 45$ μm. We define the interface Mach number to be the speed of the interface divided by the gas sound speed at the center of the bubble. The gas is compressing, its sound speed is increasing, and its velocity is directed inward radially, during the collapse. The interface speed increases monotonically during the collapse. Mach 1 is reached when the bubble radius is 1.7 μm. This leaves little time and distance for the shock amplitude and velocity to increase significantly by spherical convergence. The figure shows that the shock is not sustained, because the Mach number drops below unity at $R = 0.6$ μm. The compression of the gas between the shock and the origin (due to the pre-existing inward radial velocity) raises the sound speed faster proportionally than the interface velocity, which decreases the Mach number. We note that although a shock can be generated for interface velocities less than the speed of sound,[9] we use ‘Mach 1’ as a convenient reference value for our analyses.

The numerical simulations shown in Fig. 1a do not agree with experimental data for a sonoluminescing deuterium bubble in deuterated water.[15] Measured pulse widths are less than 15 ps, and the visible emissions are violet in color. This suggests the existence of a shock wave and central temperatures at least an order of magnitude greater than the 0.5 eV shown in Fig. 1a. The discrepancy can be explained by modelling the bubble contents differently. The bubble does not contain only pure deuterium, it also contains deuterated water vapor. The added mass of the vapor lowers the sound speed of the mixture, which makes it easier to shock. We do not know how to estimate the water vapor fraction, nor do we have an equation of state for water that is valid for rarified vapor, condensate, and compressed dense liquid. Consequently, we use our air equation of state,[6] which is valid in all these regions. It is not unreasonable to approximate the water vapor using an air equation of state, because we are interested primarily in the sound speed reduction due to added mass. It is fortuitous that the molecular weights and ionization energies of air and water vapor are similar. Figure 1b shows the calculated time dependence of the temperature at the center of the bubble, near the conclusion of the collapse of a bubble containing a mixture of 85% molar (= 44% mass fraction) deuterium and 15% molar air (≈ *deuterated water vapor*). The sound speed of the mixture at STP is 657 m/s, versus 913 m/s for pure deuterium. The final 100 ps are shown, beginning at 38.29578 μs. The minimum bubble radius (0.52 μm) occurs 36 ps after the peak temperature. The pulse width and temperature are now more consistent with the experimental data, and these results are insensitive to small changes in the molar ratios. Figure 2 (large dashed line) shows that the interface speed exceeds Mach 1 when $R = 3.8\,\mu\mathrm{m}$. The interface speed becomes subsonic at approximately the same radius as for the pure deuterium bubble, but the shock does not dissipate, because there has been enough time and distance for spherical convergence to increase the shock amplitude and velocity, so the shock reaches the origin before the interface can “communicate” with it.

The consistency of the deuterium+vapor simulation with the experimental data provides a starting point for examining practical methods to enhance the implosion. There are many parameters to vary, including the flask (size, thickness, material), liquid composition, bubble size, ambient temperature and pressure, and driving pressure (frequency, structure, and amplitude). The most practical approach is to minimize the perturbations to a standard sonoluminescing system. Consequently, we would like to identify the simplest perturbation that has a large influence. We consider pulse shaping the driving amplitude. Figure 3 (inset) shows a 5 bar triangular spike superimposed on the 1.0 ± 0.4 bar 27.6 kHz driving pressure. The center of the spike is at 16.5 μs, and its base width is 0.5 μs. The sinusoidal drive is responsible for establishing the gross system acoustics, to which sonoluminescence is extremely sensitive. We hypothesize that the spike can supply energy without affecting the mechanisms that allow sonoluminescence to occur. Preliminary experimental data[15] show that a deuterium bubble is brighter when the driving amplitude has a spike. Figure 1c shows the calculated time dependence of the temperature at the center of the bubble, due to the driving pressure shown in Fig. 3. The final 50 ps are shown, beginning at 37.6854 μs. The 2200 eV peak central temperature occurs 11 ps before the bubble reaches its minimum radius of 0.38 μm. Figure 2 (small dashed line) shows that the spike accelerates the interface to supersonic velocities early in the implosion. This provides ample time and distance for spherical convergence to increase greatly the amplitude of the shock. The relatively long implosion time and spherical convergence allow a second shock to form behind the first shock, the 230 and 2200 eV peaks shown in Fig. 1c. In general, the central temperature increases, as the spike amplitude increases, or the center of the spike occurs later in time, or the base width of the spike decreases. Although we have not investigated completely the limits of the spiked driving pressure, we have determined that the spike must rise rapidly as a function of time for its full amplitude to drive the implosion. The shape of the base of the trailing edge of the spike is not important, because this region arrives too late to influence the implosion.

Figure 3 (solid line) shows the peak temperature at the center of the innermost nine zones (indicated by circles). The dashed line shows the deuterium density (at the peak temperature) at the same locations. We excluded thermal conduction and radiant energy transport from our simulations, to simplify the analysis of the complex hydrodynamic effects on the implosion due to the spike. The effects of thermal conduction and radiant energy transport become important typically when temperatures exceed a few hundred volts, so the calculated temperatures in the innermost couple of zones somewhat over-estimate the actual values. These energy transport mechanisms must be considered in subsequent analyses.

The continuum approximation allows Eq. (1) to be solved using arbitrarily fine zoning, when the fields (T, P, ...) vary slowly over distances that are greater than fundamental physical lengths, such as the collisional mean free path. The solution loses accuracy when this criterion is violated. Every water zone satisfies this criterion, but the innermost two gas zones do not, when the peak temperatures occur (Fig. 3). The temperature gradient is large and the zone sizes are smaller than the collisional mean free path,[17] which is density and temperature dependent. Atomic transport mechanisms may be required in subsequent analyses. Consequently, we ignore the innermost two zones in the analyses that follow.

We may obtain a conservative estimate of the number of neutrons produced by the thermonuclear reaction $\mathrm{D} + \mathrm{D} \rightarrow {}^3\mathrm{He} + \mathrm{n} + 3.2\,\mathrm{MeV}$, if we ignore the innermost two zones and the energy flux from these zones into the adjacent ones. Using Fig. 3 and the formula[16]

$$\dot{N} = 0.5n^2\overline{\sigma v}, \qquad (3)$$

where $\dot{N}$, n, and $\overline{\sigma v}$ are the number of neutrons/(cc-s), the number of deuterons/cc, and the velocity-weighted D–D reaction cross section,[18] we integrate over the reaction volume and flash duration, then multiply by the number of flashes per hour (27,600 x 3600). Figure 3 shows the resulting neutron production rates <u>per hour</u> in each of the zones. We calculate a total rate of 0.1 neutron/hour, neglecting the innermost two zones.

Although the count rate is low, it should be measurable. We assume that the neutron production is coincident with the flash, so the time of arrival of the neutrons at the detector can be determined accurately. Furthermore, the energy spectrum of the neutrons is also well–defined, so temporal and energy gating of the detector can remove most of the spurious background signals.[15] We still expect to obtain a measurable signal, even after including the reductions due to the efficiency and the solid angle of the detector.

Our simulations provide the foundation for a serious attempt to attain thermonuclear fusion from a sonoluminescing bubble. It is remarkable that it appears possible theoretically. While it is true that thermonuclear fusion has a finite probability to occur in a glass of water sitting on a table, at some point more extreme conditions make the reaction rate interesting scientifically, even though it may still be small. We believe our simulations indicate that it may be possible to enter that interesting region. The main point we want to emphasize is that the spiked drive delivers a lot more energy to the center of the bubble than a purely sinusoidal drive. Consequently, our simulations indicate that the spiked drive may have the potential to supply enough energy to generate a small amount of fusion. The parameter space is large, and there are many ways to enhance the theoretical estimates. For example, the neutron rate can be increased by at least a factor of 50 if the deuterium is replaced by a mixture of deuterium and tritium.[18] Further modifications to the spike amplitude, timing, and shape may also provide enhancements. Raising the ambient pressure to increase the bubble mass may also be beneficial. At the very least, the spiked driving pressure applied to any sonoluminescing system may produce an experimental crucible that gives the general scientific community easy and inexpensive access to pressures, temperatures, and time scales that have been unattainable previously.

We thank D. Sweider and M. Moran for useful discussions. The authors also thank L. Glenn and T. Gay for reviewing the manuscript. N. Burkhard's financial and intellectual support of this research are appreciated immeasurably. This work was performed under the auspices of the U. S. Department of Energy by Lawrence Livermore National Laboratory under Contract No. W-7405-Eng-48.

References

[1] D. F. Gaitan, "An experimental investigation of acoustic cavitation in gaseous liquids," Ph. D. dissertation, University of Mississippi, (1990).

[2] D. F. Gaitan, L. A. Crum, C. C. Church, and R. A. Roy, J. Acoust. Soc. Am. 91 (1992) 3166.

[3] B. P. Barber and S. J. Putterman, Nature 352 (1991) 318.

[4] R. Hiller, S. J. Putterman, and B. P. Barber, Phys. Rev. Lett. 69 (1992) 1182.

[5] C. C. Wu and P. H. Roberts, Phys. Rev. Lett. 70 (1993) 3424.

[6] W. C. Moss, D. B. Clarke, J. W. White, and D. A. Young, Phys. Fluids 6 (1994) 2979.

[7] D. Sweider (LLNL), private communication.

[8] B. P. Barber and S. J. Putterman, Phys. Rev. Lett. 69 (1992) 3839.

[9] Ya. B. Zel'dovich and Yu. P. Raizer, ch. I, II, and III, Physics of Shock Waves and High-Temperature Hydrodynamic Phenomena (Academic, New York, 1966).

[10] J. von Neumann and R. D. Richtmyer, J. Appl. Phys. 21 (1950) 232.

[11] F. H. Ree, LLNL Report UCRL-52190 (1976).

[12] D. A. McQuarrie, ch. 6, Statistical Mechanics (Harper and Row, New York, 1976).

[13] D. A. Young, LLNL, unpublished.

[14] D. A. Young, p. 268-278, Phase Diagrams of the Elements (Univ. Calif. Press, Berkeley, 1991).

[15] M. Moran et al., LLNL, unpublished.

[16] S. Glasstone and R. H. Lovberg, ch. 2., Controlled Thermonuclear Reactions (van Nostrand Co., Inc., Princeton, 1960).

[17] L. Spitzer, Jr., ch. 5, Physics of Fully Ionized Gases (Interscience, New York, 1962).

[18] H.-S. Bosch and G. M. Hale, Nuclear Fusion 32 (1992) 611.

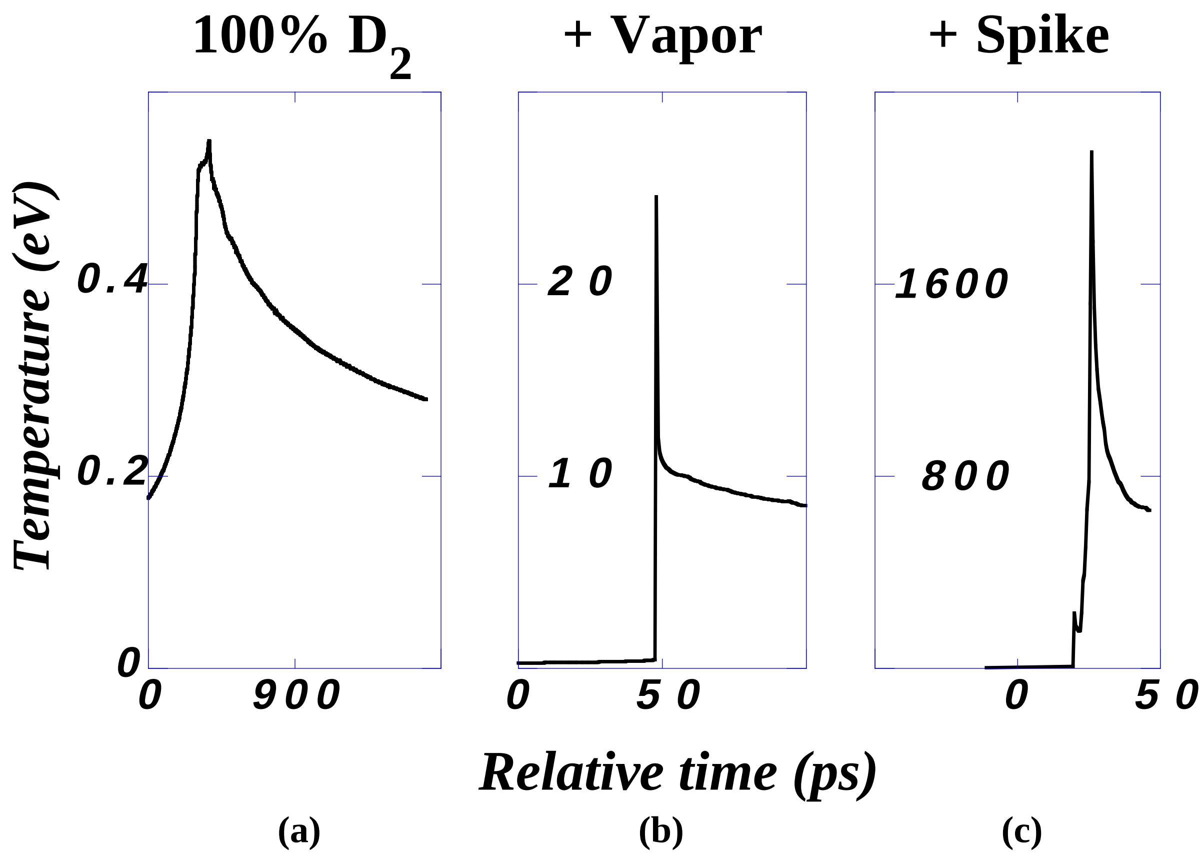

Figure 1– Temperature at the center of the bubble, as a function of time (relative to an offset origin) for (a) pure deuterium (t_0 = 38.2956 μs), (b) 85% molar deuterium with 15% molar "vapor," approximated using air (t_0 = 38.29578 μs), and (c) the mixture in (b) with a spike added to the sinusoidal driving pressure (t_0 = 37.6854 μs). The spike has a large effect on the temperature at the center of the bubble.

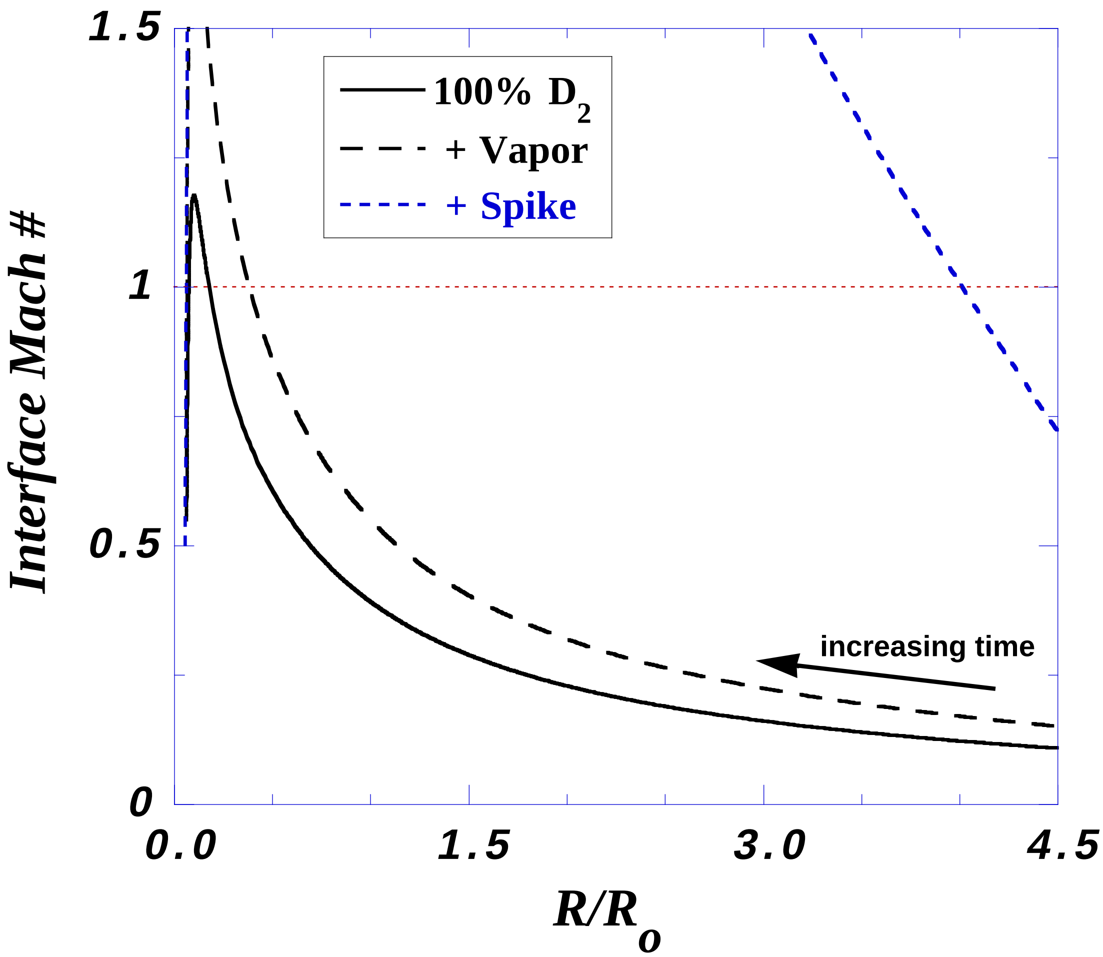

Figure 2– Radial dependence of the interface Mach number (bubble wall velocity divided by the gas sound speed at the center of the bubble) during the collapse, for the simulations shown in Fig. 1. $R_o = 10\,\mu$m. A shock is generated when the Mach number approaches unity. The spike causes a shock to be generated early in the implosion. As the shock approaches the center of the bubble, its amplitude is increased greatly by spherical convergence.

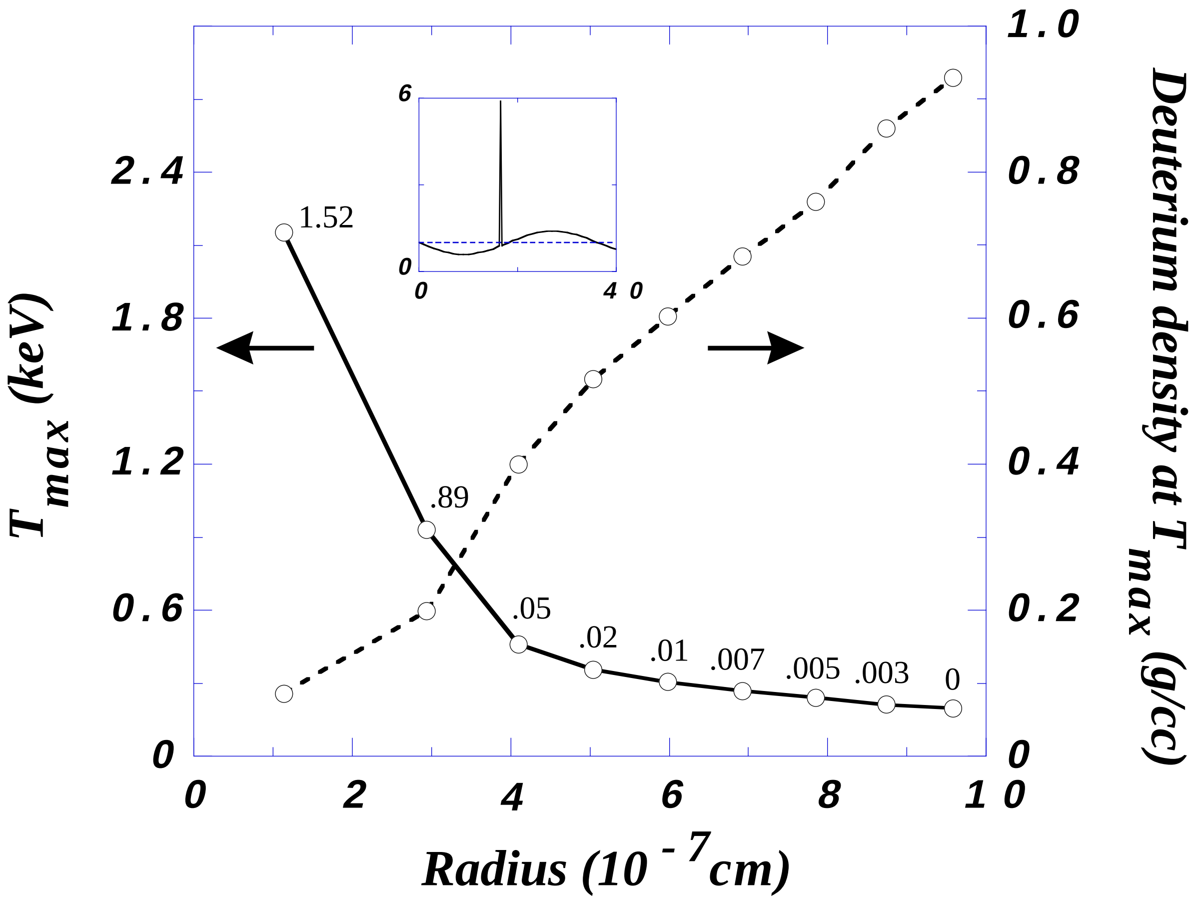

Figure 3– Calculated peak temperature (solid line) and density (dashed line) at the centers (circles) of the innermost nine zones. The 2.2 keV temperature at the center of the bubble is an over-estimate. The numbers along the solid line are the calculated number of neutrons per hour from each zone. The total rate is 0.1neutron/hour, neglecting the innermost two zones. The inset shows the driving amplitude as a function of time. A 5 bar triangular spike is superimposed on the 1.0 ± 0.4 bar 27.6 kHz sinusoidal pressure. The center of the spike is at 16.5 μs, and its base width is 0.5 μs.